Coherent effect of triple-resonant optical parametric amplification inside a cavity with injection of a squeezed vacuum field*

Di Ke(邸 克) and Zhang Jing(张 靖)†

State Key Laboratory of Quantum Optics and Quantum Optics Devices, Institute of Opto-Electronics, Shanxi University, Taiyuan 030006, *China*

(Received 6 November 2012; revised manuscript received 30 December 2012)

In theory, we study the quantum fluctuations of the subharmonic reflected field from a triple-resonant degenerate optical parametric amplifier (OPA) inside an optical cavity. We discuss two cases, where the linewidth of the harmonic field is either much narrower or broader than the subharmonic field. Since an electromagnetically-induced-transparency (EIT)-like effect can be simulated in a triple-resonant OPA, the output spectra from a triple-resonant OPA with a squeezed vacuum input may simulate the phenomenon of the response of an EIT medium for squeezed states. This scheme can be implemented with present experimental setups.

Keywords: triple-resonant optical parametric amplification, electromagnetically-induced-transparency (EIT)-like effect, squeezed vacuum field

PACS: 42.50.Ar, 42.50.Lc, 42.70.Mp **DOI:** 10.1088/1674-1056/22/9/094205

1. Introduction

The optical parametric process is an important nonlinear phenomenon and has broad applications, especially in frequency conversion and quantum information science. It can be operated with various forms and structures, such as the forms with or without cavities, using type-I or type-II phase-matched nonlinear crystal, and so on. In addition, it can also be utilized as a quantum resource to generate nonclassical and entangled states of light,[1–7] and be operated as a quantum device to manipulate quantum states of light.[8] Manipulating non-classical states, such as squeezed states and single-photon states, have been demonstrated by the optical parametric amplifier (OPA). This process is proved to be essential in the implementations of continuous variable (CV) quantum information processing, such as optimal quantum cloning machines,[9–11] quantum nondemolition measurements,[12] and all-optical CV quantum teleportation.[13]

Coherence and interference effects play an important role in determining the optical properties of quantum systems. These phenomena can be observed in the phase-sensitive OPA inside a cavity, which result from the interference between the harmonic pump field and the subharmonic field in an OPA. The destructive and constructive interferences correspond to optical parametric deamplification and amplification. Recently, a series of phenomena of classical interference in the double-resonant degenerate OPA inside an optical cavity have been studied experimentally with the injection of a coherent signal beam.[14,15] Later on, Agarwal[16] extended the results[14] to the quantum domain and studied theoretically the interferences of quantum fluctuations in an OPA inside a cavity driven by a quantized field. Recently, such quantum interference phenomenon has been demonstrated experimentally in the phase-sensitive type-I double-resonant degenerate OPA system inside an optical cavity with an injected squeezed vacuum state,[17] and both theoretically and experimentally in the phase-sensitive type-II double-resonant degenerate OPA system inside a cavity driven by a two-mode squeezed state (EPR entangled state)[18,19] and in the coupled optical driven by a squeezed vacuum state.[20] Furthermore, classical interference phenomena in the triple-resonant OPA with the injection of a coherent signal beam have been investigated theoretically[15] and experimentally,[21] in which both the subharmonic and harmonic waves simultaneously resonate inside the cavity. It is demonstrated that an electromagnetically-induced-transparency (EIT)-like effect can be simulated with a triple-resonant OPA, in which the narrow transparency window appears in the absorption spectrum and is accompanied by a very steep variation of the dispersive profile, when the cavity line-width for the harmonic wave is narrower than that for the subharmonic field.[15,21] In this paper, we investigate theoretically the quantum fluctuations of the subharmonic reflected field from a triple-resonant degenerate OPA inside an optical cavity, which is driven by the squeezed vacuum state. Spectral lineshapes due to quantum interference between the input quantum field and the generated down-converted subharmonic field are studied by scanning the length of the OPA cavity. Owing to the difference between the double-resonant and the triple-resonant OPA, the output spectral lineshapes of the squeezed vacuum field present completely different structures. Our results may simulate the phenomenon of the response of

*Project supported by the National Basic Research Program of China (Grant No. 2011CB921601), the National Natural Science Foundation of China for Excellent Research Team (Grant No. 61121064), the Specialized Research Fund for the Doctoral Program of Higher Education of China (Grant No. 20111401130001), and the Graduate Outstanding Innovation Item of Shanxi Province, China (Grant No. 20113001).

†Corresponding author. E-mail: jzhang74@yahoo.com

EIT medium for the squeezed state, which has been demonstrated experimentally through EIT in the multilevel atomic system with squeezed vacuum light.[22]

2. Theoretical model

Consider the interaction of two optical fields of frequencies ν and 2ν denoted as subharmonic and harmonic fields (the pump), which are coupled by a second-order, type-I nonlinear crystal in an optical cavity as shown in Fig. 1. The cavity is assumed to be a standing wave cavity in length L (round trip time $\tau = 2L/c$) and is resonant with both the squeezed subharmonic field and the harmonic field with dual-port of the mirrors $M_{\rm fron}$ and $M_{\rm bac}$, which forms the triple-resonant OPA. The $M_{\rm fron}$ mirror has reflectivity coefficient R_a for the subharmonic wave and high reflectivity at the harmonic wavelength. The $M_{\rm bac}$ mirror has high reflectivity at the subharmonic wavelength and reflectivity coefficient R_b for the harmonic wave. The squeezed subharmonic beam $a_{\rm in}$ is injected into the front port ($M_{\rm fron}$ mirror) of the cavity, and the pump beam $b_{\rm in}$ injected into the back port ($M_{\rm bac}$ mirror) of the cavity. The relative phase between the injected subharmonic and harmonic fields is adjusted by a movable mirror outside the cavity. The intracavity subharmonic and harmonic fields are described by a and b, and the subharmonic input and output fields are denoted by $a_{\rm in}$ and $a_{\rm ref}$, respectively.

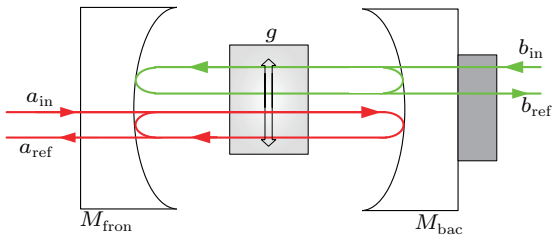

Fig. 1. (color online) Schematic of a triple-resonant optical parametric amplifier inside a standing-wave cavity.

The equations of motion for the subharmonic and harmonic fields are described by the semiclassical method as

$$\tau\frac{{\rm d}a}{{\rm d}t} = -{\rm i}\Delta_a\tau a - \gamma a + gba^* + \sqrt{2\gamma_{\rm in}^a}a_{\rm in} + \sqrt{2\rho}a_{\rm v}, \quad (1)$$

$$\tau\frac{{\rm d}b}{{\rm d}t} = -{\rm i}\Delta_b\tau b - \gamma_b b + \sqrt{2\gamma_{\rm in}^b}b_{\rm in} + \sqrt{2\rho^b}b_{\rm v}. \quad (2)$$

Here, γ is the total damping of the subharmonic field expressed as $\gamma = \gamma_{\rm in}^a + \rho$, where ρ is the decay rate for internal losses and $\gamma_{\rm in}^a = (1-R_a)/2$ is the damping associated with coupling mirror $M_{\rm fron}$, γ_b is the total damping of the harmonic field expressed by $\gamma_b = \gamma_{\rm in}^b + \rho^b$, where ρ^b is the decay rate for internal losses and similarly, $\gamma_{\rm in}^b = (1-R_b)/2$ is the damping associated with coupling mirror $M_{\rm bac}$. Vacua $a_{\rm v}$ and $b_{\rm v}$ are coupled into the subharmonic and harmonic fields through the loss ρ and ρ^b, Δ_a (Δ_b) is the detuning between the cavity-resonance frequency and the subharmonic (pump) field frequency with $\Delta_a = \Delta_b/2 = \Delta = 4\pi(L-L^{\rm res})/\tau\lambda_a$, where $L^{\rm res}$ is the cavity length at resonance and λ_a is the wavelength of the subharmonic field. The strength of the interaction is characterized by the nonlinear coupling parameter g. Equation (1) is complemented with the boundary condition $a_{\rm ref} = -a_{\rm in} + \sqrt{2\gamma_{\rm in}}a$, where $a_{\rm ref}$ is the reflected field from the front mirror. Here, equation (1) ignores the third-order term[23] describing the conversion losses due to the harmonic generation. Equation (2) ignores the coupling between the harmonic field and subharmonic field since the OPA works below the threshold and the depletion of the pump is negligible. The steady state solution (the mean value) of the harmonic intracavity field driven by a strong coherent input pump, can obtained by Eq. (2) as

$$b_{\rm st} = \frac{\sqrt{2\gamma_{\rm in}^b}|b_{\rm in}|{\rm e}^{{\rm i}\theta}}{\gamma_b + 2{\rm i}\Delta\tau}. \quad (3)$$

Since the input pump field is a strong coherent light, the mean value of the injected pump field is expressed as $\langle b_{\rm in}\rangle = {\rm e}^{{\rm i}\theta}|b_{\rm in}|$ with classical amplitude $|b_{\rm in}|$ and phase θ, where θ is the relative phase between the pump field and the signal field, which is controlled by a movable mirror outside the cavity, θ decides whether the OPA works at amplification or deamplification.

Substituting the steady-state $b_{\rm st}$ into the equation of the subharmonic field (Eq. (1)) and ignoring the high-order term, we obtain

$$\tau\frac{{\rm d}a}{{\rm d}t} = -{\rm i}\Delta\tau a - \gamma a + g\frac{\sqrt{2\gamma_{\rm in}^b}|b_{\rm in}|a^*{\rm e}^{{\rm i}\theta}}{\gamma_b + 2{\rm i}\Delta\tau} + \sqrt{2\gamma_{\rm in}^a}a_{\rm in} + \sqrt{2\rho}a_{\rm v}, \quad (4)$$

and the conjugate of Eq. (4)

$$\tau\frac{{\rm d}a^*}{{\rm d}t} = {\rm i}\Delta\tau a^* - \gamma a^* + g\frac{\sqrt{2\gamma_{\rm in}^b}|b_{\rm in}|a{\rm e}^{-{\rm i}\theta}}{\gamma_b - 2{\rm i}\Delta\tau} + \sqrt{2\gamma_{\rm in}^a}a_{\rm in}^* + \sqrt{2\rho}a_{\rm v}^*. \quad (5)$$

Since the spectra of the quadrature variances of the reflection of the subharmonic field are measured and analyzed, we take the Fourier transformation of the subharmonic field

$$a(\omega) = \frac{1}{\sqrt{2\pi}}\int {\rm d}t a(t){\rm e}^{-{\rm i}\omega t}, \quad (6)$$

$$a(-\omega)^* = \frac{1}{\sqrt{2\pi}}\int {\rm d}t a^*(t){\rm e}^{-{\rm i}\omega t}. \quad (7)$$

From Eqs. (4) and (5), we obtain

$$\begin{aligned}{\rm i}\omega\tau a(\omega) &= -{\rm i}\Delta\tau a(\omega) - \gamma a(\omega) \\ &\quad + g\frac{\sqrt{2\gamma_{\rm in}^b}|b_{\rm in}|a^*(-\omega){\rm e}^{{\rm i}\theta}}{\gamma_b + 2{\rm i}\Delta\tau} \\ &\quad + \sqrt{2\gamma_{\rm in}^a}a_{\rm in}(\omega) + \sqrt{2\rho}a_{\rm v}(\omega), \quad (8)\\ {\rm i}\omega\tau a^*(-\omega) &= {\rm i}\Delta\tau a^*(-\omega) - \gamma a^*(-\omega) \\ &\quad + g\frac{\sqrt{2\gamma_{\rm in}^b}|b_{\rm in}|a(\omega){\rm e}^{-{\rm i}\theta}}{\gamma_b - 2{\rm i}\Delta\tau} \\ &\quad + \sqrt{2\gamma_{\rm in}^a}a_{\rm in}^*(-\omega) + \sqrt{2\rho}a_{\rm v}^*(-\omega). \quad (9)\end{aligned}$$

Combining Eqs. (8) and (9), we thus obtain

$$\begin{aligned} a(\omega) = & \Big\{2g\sqrt{\gamma_{\rm in}^a\gamma_{\rm in}^b}(\gamma_b-2{\rm i}\Delta\tau)|b_{\rm in}|a_{\rm in}^*(-\omega)\,{\rm e}^{{\rm i}\theta} \\ & +2g\sqrt{\gamma_{\rm in}^b\rho}(\gamma_b-2{\rm i}\Delta\tau)|b_{\rm in}|a_{\rm v}^*(-\omega)\,{\rm e}^{{\rm i}\theta} \\ & +\sqrt{2\gamma_{\rm in}^a}(\gamma_b^2+4\Delta^2\tau^2)\big[\gamma+{\rm i}(\omega-\Delta)\tau\big]a_{\rm in}(\omega) \\ & +\sqrt{2\rho}(\gamma_b^2+4\Delta^2\tau^2)[\gamma+{\rm i}(\omega-\Delta)\tau]a_{\rm v}(\omega)\Big\} \\ & \Big/\Big\{(\gamma_b^2+4\Delta^2\tau^2)\big[\gamma^2+(\Delta^2-\omega^2)\tau^2 \\ & +2{\rm i}\omega\tau\gamma\big]-2g^2\gamma_{\rm in}^b|b_{\rm in}|^2\Big\}, \end{aligned} \tag{10}$$

$$\begin{aligned} a^*(-\omega) = & \Big\{\Big[2g\sqrt{\gamma_{\rm in}^a\gamma_{\rm in}^b}(\gamma_b+2{\rm i}\Delta\tau)|b_{\rm in}|a_{\rm in}(\omega){\rm e}^{-{\rm i}\theta} \\ & +2g\sqrt{\gamma_{\rm in}^b\rho}(\gamma_b+2{\rm i}\Delta\tau)|b_{\rm in}|a_{\rm v}(\omega){\rm e}^{-{\rm i}\theta} \\ & +\sqrt{2\gamma_{\rm in}^a}(\gamma_b^2+4\Delta^2\tau^2)[\gamma+{\rm i}(\omega+\Delta)\tau]a_{\rm in}^*(-\omega) \\ & +\sqrt{2\rho}(\gamma_b^2+4\Delta^2\tau^2)[\gamma+{\rm i}(\omega+\Delta)\tau]a_{\rm v}^*(-\omega)\Big]\Big\} \\ & \Big/\Big\{(\gamma_b^2+4\Delta^2\tau^2)\big[\gamma^2+(\Delta^2-\omega^2)\tau^2 \\ & +2{\rm i}\omega\tau\gamma\big]-2g^2\gamma_{\rm in}^b|b_{\rm in}|^2\Big\}. \end{aligned} \tag{11}$$

The quantum optical field is usually detected by the balanced homodyne detector (BHD) system, which actually measures the amplitude and phase quadratures of the optical field. The photocurrents from BHD are analyzed and recorded by using an RF spectrum analyzer. Thus, the noise spectra of the amplitude and phase quadratures at the sideband frequency ω can be investigated experimentally. The amplitude and phase quadratures of the subharmonic field are calculated and expressed by

$$\begin{aligned} X_a(\omega) &= a(\omega)+a^*(-\omega), \\ Y_a(\omega) &= -{\rm i}[a(\omega)-a^*(-\omega)]. \end{aligned} \tag{12}$$

Therefore, we thus obtain the amplitude and phase quadratures of the intracavity subharmonic field

$$\begin{aligned} X_a(\omega) = & \Big\{\Big[2g\sqrt{\gamma_{\rm in}^a\gamma_{\rm in}^b}|b_{\rm in}|(\gamma_b\cos\theta+2\Delta\tau\sin\theta) \\ & +\sqrt{2\gamma_{\rm in}^a}(\gamma_b^2+4\Delta^2\tau^2)\gamma \\ & +{\rm i}\sqrt{2\gamma_{\rm in}^a}(\gamma_b^2+4\Delta^2\tau^2)\omega\tau\Big]X_{\rm in}^a(\omega) \\ & +\Big[\sqrt{2\gamma_{\rm in}^a}(\gamma_b^2+4\Delta^2\tau^2)\Delta\tau \\ & +2g\sqrt{\gamma_{\rm in}^a\gamma_{\rm in}^b}|b_{\rm in}|(\gamma_b\sin\theta-2\Delta\tau\cos\theta)\Big]Y_{\rm in}^a(\omega) \\ & +\Big[2g\sqrt{\gamma_{\rm in}^b\rho}|b_{\rm in}|(\gamma_b\cos\theta+2\Delta\tau\sin\theta) \\ & +\sqrt{2\rho}(\gamma_b^2+4\Delta^2\tau^2)\gamma+{\rm i}\sqrt{2\rho}(\gamma_b^2 \\ & +4\Delta^2\tau^2)\omega\tau\Big]X_{\rm v}^a(\omega)+\Big[\sqrt{2\rho}(\gamma_b^2+4\Delta^2\tau^2)\Delta\tau \\ & +2g|b_{\rm in}|\sqrt{\gamma_{\rm in}^b\rho}(\gamma_b\sin\theta-2\Delta\tau\cos\theta)\Big]Y_{\rm v}^a(\omega)\Big\} \\ & \Big/\Big\{(\gamma_b^2+4\Delta^2\tau^2)\big[\gamma^2+(\Delta^2-\omega^2)\tau^2 \\ & +2{\rm i}\omega\tau\gamma\big]-2g^2\gamma_{\rm in}^b|b_{\rm in}|^2\Big\}, \end{aligned}$$

$$\begin{aligned} Y_a(\omega) = & \Big\{\Big[2g\sqrt{\gamma_{\rm in}^a\gamma_{\rm in}^b}|b_{\rm in}|(\gamma_b\sin\theta-2\Delta\tau\cos\theta) \\ & -\sqrt{2\gamma_{\rm in}^a}(\gamma_b^2+4\Delta^2\tau^2)\Delta\tau\Big]X_{\rm in}^a(\omega) \\ & +\Big[-2g\sqrt{\gamma_{\rm in}^a\gamma_{\rm in}^b}|b_{\rm in}|(\gamma_b\cos\theta+2\Delta\tau\sin\theta) \\ & +\sqrt{2\gamma_{\rm in}^a}(\gamma_b^2+4\Delta^2\tau^2)\gamma \\ & +{\rm i}\sqrt{2\gamma_{\rm in}^a}(\gamma_b^2+4\Delta^2\tau^2)\omega\tau\Big]Y_{\rm in}^a(\omega) \\ & +\Big[2g\sqrt{\gamma_{\rm in}^b\rho}|b_{\rm in}|(\gamma_b\sin\theta-2\Delta\tau\cos\theta) \\ & -\sqrt{2\rho}(\gamma_b^2+4\Delta^2\tau^2)\Delta\tau\Big]X_{\rm v}^a(\omega) \\ & +\Big[-2g\sqrt{\gamma_{\rm in}^b\rho}|b_{\rm in}|(\gamma_b\cos\theta+2\Delta\tau\sin\theta) \\ & +\sqrt{2\rho}(\gamma_b^2+4\Delta^2\tau^2)\gamma \\ & +{\rm i}\sqrt{2\rho}(\gamma_b^2+4\Delta^2\tau^2)\omega\tau\Big]Y_{\rm v}^a(\omega)\Big\} \\ & \Big/\Big\{(\gamma_b^2+4\Delta^2\tau^2)[\gamma^2+(\Delta^2-\omega^2)\tau^2 \\ & +2{\rm i}\omega\tau\gamma]-2g^2\gamma_{\rm in}^b|b_{\rm in}|^2\Big\}. \end{aligned} \tag{13}$$

According to the boundary condition $X_{\rm o}^a=\sqrt{2\gamma_{\rm in}^a}X_a-X_{\rm in}^a$ and $Y_{\rm o}^a=\sqrt{2\gamma_{\rm in}^a}Y_a-Y_{\rm in}^a$, we acquire the amplitude and phase quadratures of the output subharmonic field

$$\begin{aligned} X_{\rm o}^a(\omega) = & \Big\{\Big[2\sqrt{2}g\sqrt{\gamma_{\rm in}^b\gamma_{\rm in}^a}|b_{\rm in}|(\gamma_b\cos\theta+2\Delta\tau\sin\theta) \\ & +2\gamma_{\rm in}^a(\gamma_b^2+4\Delta^2\tau^2)\gamma+2g^2\gamma_{\rm in}^b|b_{\rm in}|^2 \\ & -(\gamma_b^2+4\Delta^2\tau^2)\Big[\gamma^2+(\Delta^2-\omega^2)\tau^2\Big] \\ & +2{\rm i}(\gamma_b^2+4\Delta^2\tau^2)\omega\tau(\gamma_{\rm in}^a-\gamma)\Big]X_{\rm in}^a(\omega) \\ & +\Big[2\gamma_{\rm in}^a(\gamma_b^2+4\Delta^2\tau^2)\Delta\tau \\ & +2\sqrt{2}g\sqrt{\gamma_{\rm in}^b\gamma_{\rm in}^a}|b_{\rm in}|(\gamma_b\sin\theta-2\Delta\tau\cos\theta)\Big]Y_{\rm in}^a(\omega) \\ & +\Big[2\sqrt{2}g|b_{\rm in}|\sqrt{\gamma_{\rm in}^a\gamma_{\rm in}^b\rho}(\gamma_b\cos\theta+2\Delta\tau\sin\theta) \\ & +2\sqrt{\gamma_{\rm in}^a\rho}(\gamma_b^2+4\Delta^2\tau^2)\gamma \\ & +2{\rm i}\sqrt{\gamma_{\rm in}^a\rho}(\gamma_b^2+4\Delta^2\tau^2)\omega\tau\Big]X_{\rm v}^a(\omega) \\ & +\Big[2\sqrt{\gamma_{\rm in}^a\rho}(\gamma_b^2+4\Delta^2\tau^2)\Delta\tau \\ & +2\sqrt{2}g\sqrt{\gamma_{\rm in}^a\gamma_{\rm in}^b\rho}|b_{\rm in}|(\gamma_b\sin\theta-2\Delta\tau\cos\theta)\Big]Y_{\rm v}^a(\omega)\Big\} \\ & \Big/\Big\{(\gamma_b^2+4\Delta^2\tau^2)\Big[\gamma^2+(\Delta^2-\omega^2)\tau^2+2{\rm i}\omega\tau\gamma\Big] \\ & -2g^2\gamma_{\rm in}^b|b_{\rm in}|^2\Big\}, \end{aligned}$$

$$\begin{aligned} Y_{\rm o}^a(\omega) = & \Big\{\Big[2\sqrt{2}g\sqrt{\gamma_{\rm in}^b\gamma_{\rm in}^a}|b_{\rm in}|(\gamma_b\sin\theta-2\Delta\tau\cos\theta) \\ & -2\gamma_{\rm in}^a(\gamma_b^2+4\Delta^2\tau^2)\Delta\tau\Big]X_{\rm in}^a(\omega) \\ & +\Big[-2\sqrt{2}g\sqrt{\gamma_{\rm in}^b\gamma_{\rm in}^a}|b_{\rm in}|(\gamma_b\cos\theta+2\Delta\tau\sin\theta) \\ & +2\gamma_{\rm in}^a(\gamma_b^2+4\Delta^2\tau^2)\gamma+2g^2\gamma_{\rm in}^b|b_{\rm in}|^2 \\ & -(\gamma_b^2+4\Delta^2\tau^2)\Big[\gamma^2+(\Delta^2-\omega^2)\tau^2\Big] \\ & +2{\rm i}(\gamma_b^2+4\Delta^2\tau^2)\omega\tau(\gamma_{\rm in}^a-\gamma)\Big]Y_{\rm in}^a(\omega) \end{aligned}$$

$$+\left[2\sqrt{2}g\sqrt{\gamma_{\rm in}^a\gamma_{\rm in}^b\rho}|b_{\rm in}|(\gamma_b\sin\theta-2\Delta\tau\cos\theta)\right.$$
$$\left.-2\sqrt{\gamma_{\rm in}^a\rho}(\gamma_b^2+4\Delta^2\tau^2)\Delta\tau\right]X_{\rm v}^a(\omega)$$
$$+\left[-2\sqrt{2}g\sqrt{\gamma_{\rm in}^a\gamma_{\rm in}^b\rho}|b_{\rm in}|(\gamma_b\cos\theta+2\Delta\tau\sin\theta)\right.$$
$$+2\sqrt{\gamma_{\rm in}^a\rho}(\gamma_b^2+4\Delta^2\tau^2)\gamma$$
$$\left.+{\rm i}2\sqrt{\gamma_{\rm in}^a\rho}(\gamma_b^2+4\Delta^2\tau^2)\omega\tau\right]Y_{\rm v}^a(\omega)\Big\}$$
$$\Big/\Big\{(\gamma_b^2+4\Delta^2\tau^2)\Big[\gamma^2+(\Delta^2-\omega^2)\tau^2$$
$$+2{\rm i}\omega\tau\gamma\Big]-2g^2\gamma_{\rm in}^b|b_{\rm in}|^2\Big\}. \quad (14)$$

The fluctuation variances of the amplitude and phase quadratures of the output subharmonic field are expressed as

$$\langle\delta^2X_{\rm o}^a(\omega)\rangle = \Big\{\Big(\Big[2\sqrt{2}g\gamma_{\rm in}^a\sqrt{\gamma_{\rm in}^b}|b_{\rm in}|(\gamma_b\cos\theta+2\Delta\tau\sin\theta)$$
$$+2\gamma_{\rm in}^a(\gamma_b^2+4\Delta^2\tau^2)\gamma-(\gamma_b^2+4\Delta^2\tau^2)$$
$$\Big[\gamma^2+(\Delta^2-\omega^2)\tau^2\Big]+2g^2\gamma_{\rm in}^b|b_{\rm in}|^2\Big]^2$$
$$+\Big[2(\gamma_b^2+4\Delta^2\tau^2)\omega\tau(\gamma_{\rm in}^a-\gamma)\Big]^2\Big)\langle\delta^2X_{\rm in}^a(\omega)\rangle$$
$$+\Big[2\gamma_{\rm in}^a(\gamma_b^2+4\Delta^2\tau^2)\Delta\tau+2\sqrt{2}g\sqrt{\gamma_{\rm in}^b}$$
$$\times\gamma_{\rm in}^a|b_{\rm in}|(\gamma_b\sin\theta-2\Delta\tau\cos\theta)\Big]^2\langle\delta^2Y_{\rm in}^a(\omega)\rangle$$
$$+\Big(\Big[2\sqrt{2}g\sqrt{\gamma_{\rm in}^a\gamma_{\rm in}^b\rho}|b_{\rm in}|(\gamma_b\cos\theta+2\Delta\tau\sin\theta)$$
$$+2\sqrt{\gamma_{\rm in}^a\rho}(\gamma_b^2+4\Delta^2\tau^2)\gamma\Big]^2$$
$$+\Big[2\sqrt{\gamma_{\rm in}^a\rho}(\gamma_b^2+4\Delta^2\tau^2)\omega\tau\Big]^2\Big)\langle\delta^2X_{\rm v}^a(\omega)\rangle$$
$$+\Big[2\sqrt{\gamma_{\rm in}^a\rho}(\gamma_b^2+4\Delta^2\tau^2)\Delta\tau+2\sqrt{2}g\sqrt{\gamma_{\rm in}^a\gamma_{\rm in}^b\rho}$$
$$\times|b_{\rm in}|(\gamma_b\sin\theta-2\Delta\tau\cos\theta)\Big]^2\langle\delta^2Y_{\rm v}^a(\omega)\rangle\Big\}$$
$$\Big/\Big\{\Big[(\gamma_b^2+4\Delta^2\tau^2)(\gamma^2+(\Delta^2-\omega^2)\tau^2)$$
$$-2g^2\gamma_{\rm in}^b|b_{\rm in}|^2\Big]^2+\Big[2(\gamma_b^2+4\Delta^2\tau^2)\omega\tau\gamma\Big]^2\Big\},$$
$$\langle\delta^2Y_{\rm o}^a(\omega)\rangle = \Big\{\Big[2\sqrt{2}g\sqrt{\gamma_{\rm in}^b}\gamma_{\rm in}^a|b_{\rm in}|(\gamma_b\sin\theta-2\Delta\tau\cos\theta)$$
$$-2\gamma_{\rm in}^a(\gamma_b^2+4\Delta^2\tau^2)\Delta\tau\Big]^2\langle\delta^2X_{\rm in}^a(\omega)\rangle$$
$$+\Big(\Big[-2\sqrt{2}g\sqrt{\gamma_{\rm in}^b}\gamma_{\rm in}^a|b_{\rm in}|(\gamma_b\cos\theta+2\Delta\tau\sin\theta)$$
$$+2\gamma_{\rm in}^a(\gamma_b^2+4\Delta^2\tau^2)\gamma+2g^2\gamma_{\rm in}^b|b_{\rm in}|^2$$
$$-(\gamma_b^2+4\Delta^2\tau^2)\Big[\gamma^2+(\Delta^2-\omega^2)\tau^2\Big]\Big]^2$$
$$+\Big[2(\gamma_b^2+4\Delta^2\tau^2)\omega\tau(\gamma_{\rm in}^a-\gamma)\Big]^2\Big)\langle\delta^2Y_{\rm in}^a(\omega)\rangle$$
$$+\Big[2\sqrt{2}g\sqrt{\gamma_{\rm in}^a\gamma_{\rm in}^b\rho}|b_{\rm in}|(\gamma_b\sin\theta-2\Delta\tau\cos\theta)$$
$$-2\sqrt{\gamma_{\rm in}^a\rho}(\gamma_b^2+4\Delta^2\tau^2)\Delta\tau\Big]^2\langle\delta^2X_{\rm v}^a(\omega)\rangle$$
$$+\Big(\Big[2\sqrt{\gamma_{\rm in}^a\rho}(\gamma_b^2+4\Delta^2\tau^2)\gamma$$
$$-2\sqrt{2}\sqrt{\gamma_{\rm in}^a\gamma_{\rm in}^b\rho}g|b_{\rm in}|(\gamma_b\cos\theta+2\Delta\tau\sin\theta)\Big]^2$$
$$+\Big[2\sqrt{\gamma_{\rm in}^a\rho}(\gamma_b^2+4\Delta^2\tau^2)\omega\tau\Big]^2\Big)\langle\delta^2Y_{\rm v}^a(\omega)\rangle\Big\}$$
$$\Big/\Big\{\Big[(\gamma_b^2+4\Delta^2\tau^2)(\gamma^2+(\Delta^2-\omega^2)\tau^2$$
$$-2g^2\gamma_{\rm in}^b|b_{\rm in}|^2\Big]^2+\Big[2(\gamma_b^2+4\Delta^2\tau^2)\omega\tau\gamma\Big]^2\Big\}. \quad (15)$$

Here, $\langle\delta^2X_{\rm v}^a(\omega)\rangle=\langle\delta^2Y_{\rm v}^a(\omega)\rangle=1$ as it is the vacuum input field.

The cavity linewidth is given by $W=\Delta_{\rm FSR}/F$, where F is the cavity finesse and $F=1/\gamma_{\rm total}$. In the following, we will discuss two cases for triple-resonant degenerate OPA: $\gamma_{\rm in}^a+\rho\ll\gamma_{\rm in}^b+\rho^b$ (the linewidth of the harmonic field is much larger than that of the subharmonic field), and the contrary case $\gamma_{\rm in}^a+\rho\gg\gamma_{\rm in}^b+\rho^b$. Here, the triple-resonant OPA is operated below the threshold $\beta_{\rm th}^{\rm in}=\gamma\gamma_b/(g\sqrt{2\gamma_{\rm in}^b})$.

3. Coherent effect of triple-resonant OPA with injection of a squeezed vacuum field in different conditions

Case 1 The linewidth of the harmonic field is much larger than the linewidth of the subharmonic field. We make $\gamma_{\rm in}^a=0.04$, $\rho=0.005$, $\gamma_{\rm in}^b=0.16$, and $\rho^b=0.001$, and first study the spectral lineshapes of the OPA with a injecting vacuum state ($\langle\delta^2X_{\rm in}^a(\omega)\rangle=\langle\delta^2Y_{\rm in}^a(\omega)\rangle=1$). When the pump field is blocked, the spectral feature of the reflected signal field is the same as shot noise limit (SNL), as shown in the Figs. 2(a) and 2(b). When the pump beam is turned on, the reflected spectrum near cavity resonance is changed by OPA. One quadrature (in phase) component is deamplified at resonance and becomes squeezed (below SNL). The other quadrature (out of phase) component is amplified and becomes antisqueezed (above SNL). Thus there is a dip (peak) of the reflected spectrum at the $\Delta=0$ as shown in the Fig. 2(c) (Fig. 2(d)). The spectrum just outside the resonant appears two peaks as shown in Fig. 2(c), which indicates that small amplification can occur when the cavity is detuned from the resonance even for the deamplified operation at resonance. On the contrary, the spectrum of the other quadrature component has two dips (Fig. 2(d)) just outside the resonance. The spectra at the detuning far from the cavity resonance correspond to the noise of input field as the input field does not interact with the pump field through the nonlinear crystal.

Now, we study the case of injecting a squeezed vacuum. When the pump beam is blocked and scanning the length of the OPA cavity, let us look at the squeezed quadrature of the reflected beam, as shown in Fig. 3(a), by choosing the phase of local beam relative to the input squeezed vacuum state $\phi=0$. The center part of the reflected spectrum is modified by the optical cavity. The point at resonance is almost equal to the input squeezing and the part just outside the resonant appears as two peaks which corresponds the input

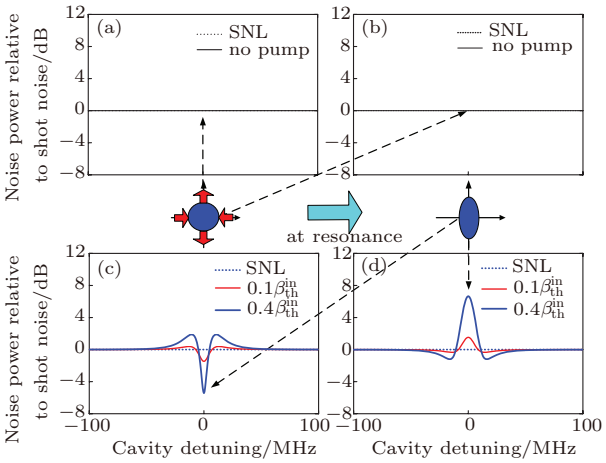

Fig. 2. (color online) The noise fluctuation spectra of the subharmonic reflection field from the OPA cavity injected with the vacuum states when the linewidth of harmonic field is much larger than the subharmonic field. Quantum noise is analyzed at the sideband frequency of $\omega = 2$ MHz. (a) and (b) show the reflection spectra of amplitude (in phase) and phase (out of phase) components without the pump beam; (c) and (d) show the reflection spectra of amplitude (in phase) and phase (out of phase) components with the input pump power at $0.1\beta_{th}^{in}$ and $0.4\beta_{th}^{in}$.

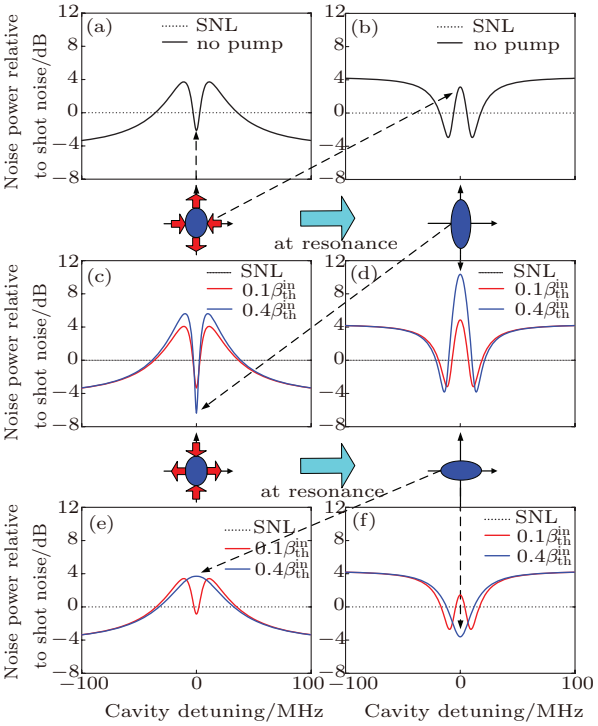

Fig. 3. (color online) The noise fluctuation spectra of the subharmonic reflection field from the OPA cavity injected with the squeezed vacuum beam, in which the linewidth of the harmonic field is much larger than the subharmonic field. The squeezing level of the input field is -4.34 dB and quantum noise is analyzed at the sideband frequency of 2 MHz. (a) and (b) without the pump beam; (c) and (d) show the reflection spectra of amplitude (in phase) and phase (out of phase) components for fixing the relative phase $\theta = 0$ between the input pump beam and signal beam; (e) and (f) show the reflection spectra of amplitude and phase components for fixing the relative phase $\theta = \pi/2$ between the input pump beam and the signal beam.

anti-squeezing. The spectra at the detuning far from the cavity resonance return back the input squeezing. Looking at the antisqueezed quadrature of the reflected beam, the spectral lineshape is just opposite to the squeezed quadrature as shown in Fig. 3(b). This spectral shape is induced by the absorption and dispersion properties of the empty cavity.[24–28]

When the pump beam is turned on and the relative phase between the input pump beam, and signal beam is tuned to be $\theta = 0$, we can see the spectral lineshapes of the reflected field as shown in Figs. 3(c) and 3(d). Let us look at the squeezed quadrature of the reflected beam from the OPA, as shown in Fig. 3(c), by choosing the phase of local beam relative to the input squeezed vacuum state $\phi = 0$. The reflected spectrum at resonance is deamplified by the OPA, so the squeezing is further increased. Two peaks just outside the resonant are amplified by the OPA. On the other hand, the reflected spectrum for the antisqueezed quadrature at resonance is amplified by the OPA, so the fluctuation is increased, as shown in Fig. 3(d). Two dips just outside the resonance are also changed.

Now, let us examine the situation of the relative phase $\phi = \pi/2$. The reflected spectrum for the squeezed quadrature at resonance is amplified by the OPA, so the squeezing is decreased as shown in the Fig. 3(e). Meanwhile, the antisqueezed quadrature at resonance is deamplified by the OPA. These above theoretical results are consistent with the experimental observation for the double-resonant degenerate OPA.[17]

Case 2 The linewidth of the harmonic field is much narrower than the linewidth of the subharmonic field. We set $\gamma_{in}^{a} = 0.04$, $\rho = 0.005$, $\gamma_{in}^{b} = 0.01$, and $\rho^{b} = 0.001$. First, we consider vacuum as the signal field injecting into the OPA, as shown in Figs. 4(a)–4(d). The spectral lineshapes of the reflected field generated by OPA (Figs. 4(c) and 4(d)) are similar with those in case 1 (Figs. 2(c) and 2(d)), however, they are much narrower compared with case 1 due to the narrower linewidth of the harmonic field.

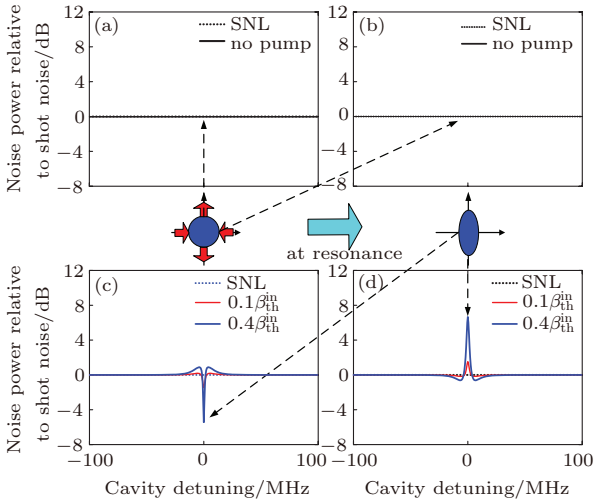

Fig. 4. (color online) The noise fluctuation spectra of the subharmonic reflection field from the OPA cavity injected by the vacuum state when the linewidth of subharmonic field is much larger than that of the harmonic field. Quantum noise is analyzed at the sideband frequency of 2 MHz. (a) and (b) without the pump beam; (c) and (d) with the input pump power at $0.1\beta_{th}^{in}$ and $0.4\beta_{th}^{in}$.

When injecting a squeezed vacuum field, the spectral lineshapes without the pump light (Figs. 5(a) and 5(b)) are the same as case 1. When the pump beam is turned on and the relative phase between the input pump beam and squeezed light is tuned to be $\theta = 0$, the spectral lineshapes of the reflected field are shown in the Figs. 5(c) and 5(d). Figures 5(e) and 5(f) show the spectral lineshapes of the reflected field with the relative phase $\theta = \pi/2$. It can be seen that the spectral lineshape of the subharmonic reflected field in the region of the larger linewidth of harmonic field is determined by the absorption and dispersion properties of the empty cavity. However, the spectra of the subharmonic reflected field located inside the linewidth of harmonic field appear a narrow peak induced by the optical parametric process for the narrower linewidth of harmonic field. Since the narrow absorption and dispersion of the pump field are introduced into the subharmonic field via the parametric interaction in triple-resonant OPA, the reflected spectra of the subharmonic field present narrow peak in the center. Note that the relative phase between the input pump beam and squeezed light plays an important role in determing the spectral lineshape of the subharmonic reflected field.

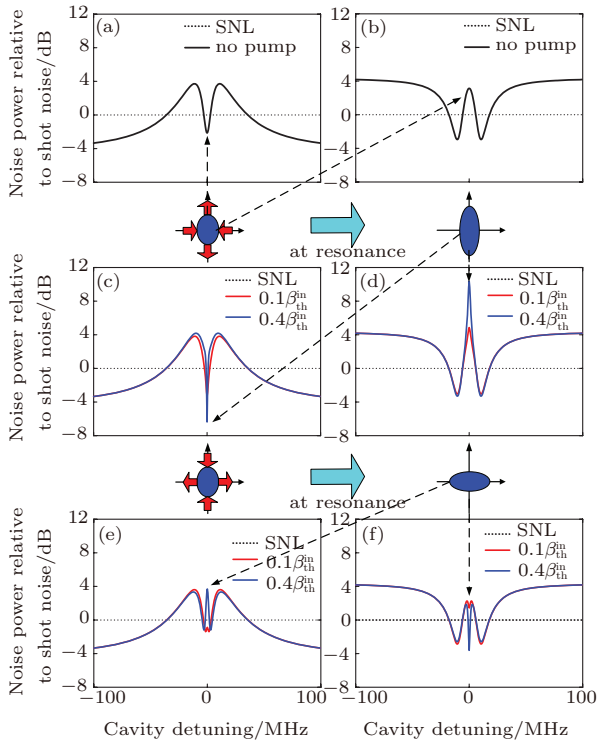

Fig. 5. (color online) The noise fluctuation spectra of the subharmonic reflection field from the OPA cavity injected with the input squeezed beam, in which the linewidth of the harmonic field is much narrower than the linewidth of the subharmonic field. The squeezing level of the input field is −4.34 dB and quantum noise is analyzed at the sideband frequency of 2 MHz. (a) and (b) without the pump beam; (c) and (d) show the reflection spectra of amplitude and phase components for fixing the relative phase $\theta = 0$ between the input pump beam and signal beam; (e) and (f) show the reflection spectra of amplitude and phase components for fixing the relative phase $\theta = \pi/2$ between the input pump beam and the signal beam.

4. Conclusion

We have theoretically investigated the quantum coherence between the input squeezed vacuum field and the generated quantum field from a triple-resonant OPA inside a cavity. The output spectra of the subharmonic field were compared between two cases: the linewidth of the harmonic field is either much narrower or broader than the linewidth of the subharmonic field. It has been demonstrated that EIT-like effect can be simulated in a triple-resonant OPA when the cavity linewidth for the harmonic wave is narrower than that for the subharmonic field.[15,21] Thus the result presented above simulated the phenomenon of the response of an EIT medium for the input squeezed state, however, it possessed many new characteristics. This scheme can be implemented with the current experimental setups.[17,21] This work would have many important applications in the manipulation of quantum fluctuation and quantum information processing.

References

[1] Furusawa A, Sørensen J L, Braunstein S L, Fuchs C A, Kimble H J and Polzik E S 1998 *Science* **282** 706
[2] Bowen W P, Treps N, Buchler B C, Schnabel R, Ralph T C, Bachor H A, Symul T and Lam P K 2003 *Phys. Rev. A* **67** 032302
[3] Jia X J, Su X L, Pan Q, Gao J, Xie C D and Peng K C 2004 *Phys. Rev. Lett.* **93** 250503
[4] Takei N, Yonezawa H, Aoki T and Furusawa A 2005 *Phys. Rev. Lett.* **94** 220502
[5] Ou Y, Pereira S F, Kimble H J and Peng K C 1992 *Phys. Rev. Lett.* **68** 3663
[6] Zhang Y, Wang H, Li X, Jing J, Xie C D and Peng K C 2000 *Phys. Rev. A* **62** 023813
[7] D'Auria V, Fornaro S, Porzio A, Solimeno S, Olivares S and Paris M G A 2009 *Phys. Rev. Let.* **102** 020502
[8] Zhao D M, Li Z G, Guo Y Q, Li G, Wang J M and Zhang T C 2010 *Acta Phys. Sin.* **59** 6231 (in Chinese)
[9] Lamas L A, Simon C, Howell J C and Bouwmeester D 2002 *Science* **296** 712
[10] Martini F D, Pelliccia D and Sciarrino F 2004 *Phys. Rev. Lett.* **92** 067901
[11] D'Ariano G M, Martini F D and Sacchi M F 2001 *Phys. Rev. Lett.* **86** 914
[12] Bruckmeier R, Schneider K, Schiller S and Mlynek J 1997 *Phys. Rev. Lett.* **78** 1243
[13] Ralph T C 1999 *Opt. Lett.* **24** 348
[14] Ma H L, Ye C G, Wei D and Zhang J 2005 *Phys. Rev. Lett.* **95** 233601
[15] Ye C G and Zhang J 2006 *Phys. Rev. A* **73** 023818
[16] Agarwal G S 2006 *Phys. Rev. Lett.* **97** 023601
[17] Zhang J, Ye C G, Gao F and Xiao M 2008 *Phys. Rev. Lett.* **101** 233602
[18] Chen H X and Zhang J 2009 *Phys. Rev. A* **79** 063826
[19] Shang Y N, Jia X J, Shen Y, Xie C D and Peng K C 2010 *Opt. Lett.* **35** 853
[20] Di K, Xie C D and Zhang J 2011 *Phys. Rev. Lett.* **106** 153602
[21] Ye C G and Zhang J 2008 *Opt. Lett.* **33** 1911
[22] Akamatsu D, Akiba K and Kozuma M 2004 *Phys. Rev. Lett.* **92** 203602
[23] Schiller S, Kohler S, Paschotta R and Mlynek J 1995 *Appl. Phys. B* **60** 77
[24] Levenson M D, Shelby M R and Perlmutter S H 1985 *Opt. Lett.* **10** 514
[25] Galatola P, Lugiato L A, Porreca M G, Tombesic P and Leuchs G 1991 *Opt. Commun.* **85** 95
[26] Zhang J, Zhang T C, Zhang K S, Xie C D and Peng K C 2000 *J. Opt. Soc. Am. B* **17** 1920
[27] Zavatta A, Marin F and Giacomelli G 2002 *Phys. Rev. A* **66** 043805
[28] Sun W H, Chen X S and Du S D 2005 *Chin. Phys. Lett.* **22** 2812